Middle East Journal of Science

https://dergipark.org.tr/mejs
e-ISSN:2618-6136

MEJS

Research Article

INVESTIGATION OF Pd@*g*-C_3N_4/TiO_2 NANOPARTICLES AS PHOTOCATALYST IN THE DEGRADATION OF METHYLENE BLUE UNDER VISIBLE LIGHT IRRADIATION

***Halil İbrahim ÖNAL*[1]** ***[*]Feyyaz DURAP*[2]**

[1]Dicle University, Science Faculty, Department of Chemistry, 21280-Diyarbakır, Turkey
[2]Dicle University, Science Faculty, Department of Chemistry, 21280-Diyarbakır, Turkey
[*]Corresponding author: fdurap@dicle.edu.tr

Abstract: *In the present study, the efficiency of Pd@g-C_3N_4/TiO_2 NPs as photocatalysts on the degradation of organic pollutant methylene blue (MB) dye under visible light has been investigated. A traditional one-step impregnation-reduction method was used for the preparation of photocatalysts. Pd@g-C_3N_4/TiO_2 NPs were characterized by several techniques such as FT-IR, DR/UV-Vis, SEM-EDX, TEM, P-XRD, and XPS analyses. The photocatalytic performance of Pd@g-C_3N_4/TiO_2 NPs was evaluated for the degradation of MB dye under visible light irradiation. Among different loadings of Pd (0.3, 0.5, and 0.7 %), the 0.5% loading Pd@g-C_3N_4/TiO_2 NPs showed the highest catalytic activity. The results revealed an enhancement in the visible light photocatalytic activity of g-C_3N_4/TiO_2 when it was coupled with Pd in the composite. Compared with pure g-C_3N_4/TiO_2, the Pd@ g-C_3N_4/TiO_2 hybrid photocatalyst exhibited enhanced visible-light photoactivity, which was approximately three times higher than that of pure g-C_3N_4/TiO_2.*

Keywords: *Pd, g-C_3N_4/TiO_2, Methylene Blue, Photocatalyst, Nanoparticle.*

Received: October 1, 2021 Accepted: December 20,2021

1. Introduction

One of the main factors for serious environmental problems is the release of several hazardous organic dyes from textile industries in wastewater, which is concerned with human health and the environment due to the toxicity and the carcinogenic effect of these dyes [1]. In this context, we can list the process generally used to remove these toxic dyes from water as adsorption [2], chemical precipitation [3], sedimentation [4], biological membranes [5], ion exchange [6], and electrochemical [7]. However, these methods have several disadvantages such as they usually proceed slowly, require expensive equipment and require further elimination [8]. Photocatalytic methods can increase the use of solar energy and reduce pollutants in wastewater [9]. This issue is important both in terms of environmental protection and shows the importance of using a photocatalyst in terms of economy and time. In recent years, nano-sized semiconductors such as TiO_2 [10, 11, 12], ZnO [13], Fe_2O_3 [14] and CdS [15] have yielded successful results in dye removal, which shows that they exhibit high photocatalytic reactivity.

Graphitic carbon nitride (*g*-C_3N_4) is a photocatalytic support material that has recently attracted attention with its advantageous stable physicochemical properties (absorption at 400-450 nm and narrow energy band gap) but it has disadvantages such as high recombination rate, which reduces its catalytic activity. [16,17,18,19]. Furthermore, number of reports have shown that TiO_2 exhibits robust photocatalytic activity, although its absorption efficiency for visible light is greatly limited due to its

wide band gap (3.2 eV) [20, 21, 22, 23]. Among the developed photocatalytic systems, *g*-C_3N_4/TiO_2 composites with a high specific surface area and special heterostructure were prominent in this pursuit due to their easy synthesis, stronger visible light activity and higher electron transfer rate [24, 25, 26, 27]. Moreover, it has been proven that the noble metal palladium (Pd) can effectively improve the visible light absorption rate of composite materials, as it has abundant vacant orbitals that effectively promote electron transfer in composite materials. [28, 29, 30, 31].

In this respect, we prepared Pd@*g*-C_3N_4-TiO_2 nano heterostructured catalysts using a conventional one-step impregnation-reduction method. The results showed that these catalyst systems present excellent photocatalytic performance for methylene blue (MB) degradation under visible light, which demonstrates a promising strategic approach in the field of photocatalysis. The newly prepared Pd@*g*-C_3N_4/TiO_2 NPs were characterized by FT-IR, DR/UV-Vis, SEM-EDX, TEM, P-XRD, and XPS analyses.

2. Materials and Methods

2.1. Materials

Palladium Nitrate ($Pd(NO_3)_2$).$2H_2O$ (99%), Titanium (IV) oxide (anatase, nanopowder <25 nm particle size (99,7%), tetramethylthionine chloride (Methylene Blue; MB; $C_{16}H_{18}ClN_3SH_2O$), sodium borohydrate ($NaBH_4$), Ethanol (C_2H_5OH), Methanol (CH_3OH) were purchased from Sigma Aldrich® and Urea (CH_4N_2O) were purchased from Merck. All glassware and magnetic stir sticks were washed with acetone, rinsed profusely with ethanol and furnace dried.

2.2. Synthesis of g-C_3N_4 and g-C_3N_4/TiO_2 Composite

The *g*-C_3N_4 (CN)[32] and g-C_3N_4/TiO_2[33] composite was prepared by using well-established procedures of which the details were given in recent publications.

2.3. Preparation of Pd@g-C_3N_4/TiO_2

The Pd@*g*-C_3N_4/TiO_2 catalyst was synthesized by conventional impregnation-reduction steps [34]. For this, 5.0 mL of an aqueous solution containing $Pd(NO_3)$ (2.50 mg, 9.38 μmol Pd) and *g*-C_3N_4/TiO_2 (0.2g) was stirred for 2 hours. A fresh 1.0 mL aqueous solution of $NaBH_4$ (5.43 mg, 0.14 mmol) was then added dropwise to this mixture and stirred under ambient conditions for half an hour. The final product was washed with copious amounts of water and ethanol (2x20 mL), filtered on filter paper and dried in an oven at 353 K. As a result, the Pd@*g*-C_3N_4/TiO_2 catalyst was obtained as gray color powder.

2.4. Characterization Methods

P-XRD patterns were obtained with a Rigaku Ultima-III X-ray diffractometer at 40 kV and 35 mA using Cu Ka radiation (k = 1.54059 A). For TEM analysis, diluted suspensions of the samples were prepared and the solvent was dried after dropping onto the carbon TEM grid. SEM analyses were performed on Zeiss Sigma 300. XPS patterns were performed on a Specs-Flex XPS with a photoelectron take-off angle of 45^0. The FT-IR spectra of the samples were taken on a Cary 630 FTIR spectrometer. DR/UV–Vis analyses were performed using Shimadzu UV-3600 Plus device.

2.5. Photocatalytic Tests

The photocatalytic degradation efficiency of the prepared photocatalyst was assessed by using methylene blue dye under UV-Vis light irradiation. A 300W Tungsten halogen lamp was used as a visible light source in this photocatalytic system. An experiment was carried out by adding 10 mg of the prepared catalysts to 30 mL of methylene blue aqueous solutions (7 μg/mL) in a cooling water-jacketed Pyrex glass reactor vessel. The solution was stirred in the dark (30 min) to reach an adsorption-desorption equilibrium between the MB and the catalyst surface. A certain amount of sample (2mL) was taken from the reactor vessel and the catalyst was removed by centrifugation (4000 rpm, 6 minutes). Changes in MB concentrations in solution were analyzed using a Cary 100 Bio UV–Vis spectrophotometer at maximum absorption (λ =664 nm) at room temperature.

The photodegradation efficiency (η) and the apparent pseudo-first-order rate constant (kapp) were determined by the following equation:

$$\eta = \frac{C_0 - C}{C_0}\ x100 \quad (1)$$

$$ln\frac{C_0}{C} = k_{app}t \quad (2)$$

C_0 in the equation is the initial concentration and C is the methylene blue concentration as a function of irradiation time t.

3. Results and Discussion

3.1. The Preparation and Characterization of Pd@*g*-C_3N_4/TiO_2 Nanocomposite

Before the preparation of Pd@g-C_3N_4/TiO_2 catalyst, first g-C_3N_4 and then g-C_3N_4/TiO_2 support materials were prepared by using a modified version of the method given in the literature[40]. The g-C_3N_4/TiO_2 support material was evidenced by FT-IR spectroscopy. FT-IR data were collected for the TiO_2, *g*-C_3N_4, and *g*-C_3N_4/TiO_2 structures as seen in Figure 1. The presence of g-C_3N_4 and *g*-C_3N_4/TiO_2 nanocomposites has been observed through FT-IR spectroscopy. Strong peaks observed at 1238, 1328, and 1573 cm^{-1} for pure g-C_3N_4 are attributed to the typical stretching vibration of C-N heterocycles and a sharp peak at 806 cm^{-1} is related to the characteristic stretching vibration of triazine units. The broad peak in the range 3100-3300 cm^{-1} is assigned to the stretching vibration of N-H bonds of amines (-NH_2 and =NH)[35,36]. The wide absorption peak at 400-700 cm^{-1} corresponds to the Ti-O stretching and Ti-O-Ti bridging stretching vibrations of pure TiO_2 [37, 38]. In addition, the peaks corresponding to bending and stretching vibrations of the O-H group were observed at 1630 and 3500 cm^{-1}. The spectrum of Pd@*g*-C_3N_4-TiO_2 catalyst was similar to that of *g*-C_3N_4-TiO_2 composite and also showed all the peaks of g-C_3N_4 and TiO_2.

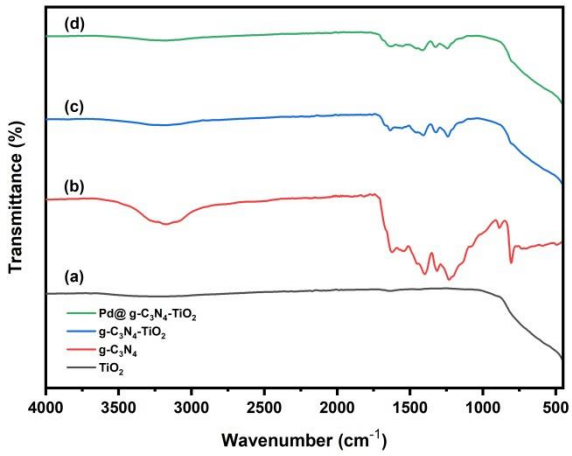

Figure 1. FT-IR spectra of TiO_2 (a), g-C_3N_4 (b), g-C_3N_4/TiO_2 (c) Pd@*g*-C_3N_4-TiO_2 (d).

In order to determine the optical properties of the Pd@*g*-C_3N_4/TiO_2 nanocatalyst, the UV-Vis diffuse reflectance spectral analysis of TiO_2, *g*-C_3N_4, and *g*-C_3N_4/TiO_2 was carried out, and the results are shown in Figure 2. As seen in Figure 2, the absorption sharp edges of TiO_2, *g*-C_3N_4, and *g*-C_3N_4/TiO_2 composite were found to be around 391, 425, and 412 nm, respectively. In addition, band gap values (Eg) of pure TiO_2, pure g-C_3N_4, and g-C_3N_4/TiO_2 composite were determined as ~ 3.08, 2.81, and 2.84 eV, respectively. In conclusion, the *g*-C_3N_4/TiO_2 nanocomposite exhibited enhanced absorption in the visible region compared to TiO_2 due to the synergistic effect between TiO_2 and g-C_3N_4. It can be seen that the bandgap of TiO_2 decreases with the addition of *g*-C_3N_4. [39].

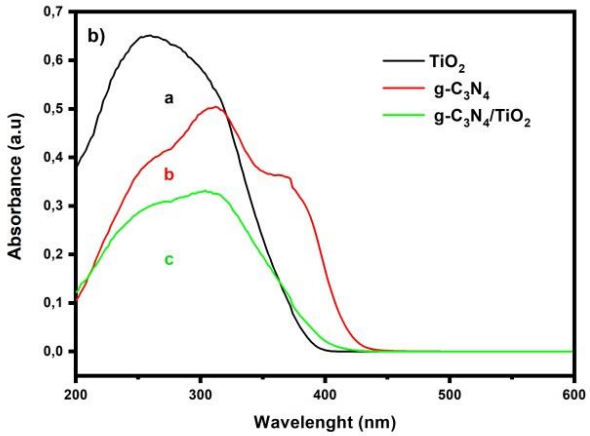

Figure 2. UV–Vis Diffuse Reflectance spectra of TiO_2 (a), *g*-C_3N_4 (b), and *g*-C_3N_4/TiO_2 composite (c)

Afterward, Pd@*g*-C_3N_4/TiO_2 nanocatalyst was simply and reproducibly prepared by following the procedure [40], Pd@*g*-C_3N_4/TiO_2 nanocatalyst was obtained as powders and characterized by P-XRD, XPS, SEM-EDX, and TEM.

The XRD patterns for fresh *g*-C_3N_4/TiO_2 composite and Pd@*g*-C_3N_4/TiO_2 photocatalyst samples are shown as a pattern in Figure 3. All the samples show the diffraction peaks of TiO_2 with 2θ values which depict the anatase phase of TiO_2 (JCPDS card No. 21–1272) and rutile phase (JCPDS card No. 21-1276) as shown in Figure 3. The one diffraction peak of *g*-C_3N_4 overlapped with the peak of the rutile phase at 27.5° (110) planes. Moreover, the diffraction peaks of Pd can only be observed

when the loading of Pd is 5% or more than 5 wt% with 2θ values of 40.2° (111), 48.0° (200), and 68.8° (220) that corresponds to the presence of Pd (JCPDS 05-0681)[41,42].

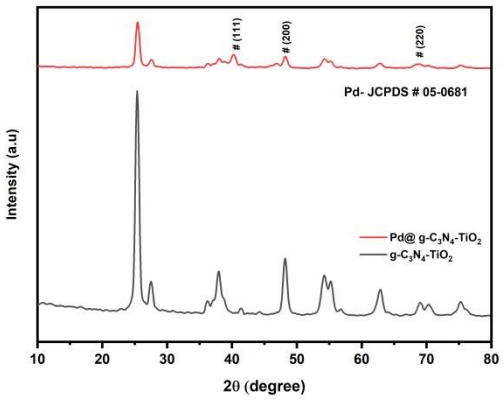

Figure 3. XRD patterns of *g*-C_3N_4/TiO_2 composite and Pd@*g*-C_3N_4/TiO_2 photocatalyst.

The surface elemental composition of the Pd@*g*-C_3N_4/TiO_2 nanocatalyst was investigated by using XPS analysis. The XPS spectrum of Pd@*g*-C_3N_4/TiO_2 taken as a survey scan is depicted in Figure 4. As seen in this spectrum, obtained signals disclose that the surface composition consists of Ti, Pd, N, C, and O.

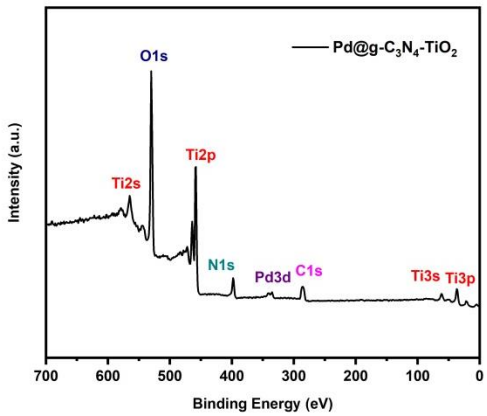

Figure 4. (a) Survey scan XPS spectrum of Pd@g-C_3N_4/TiO_2

The morphology and nanostructure of samples (*g*-C_3N_4, TiO_2, *g*-C_3N_4/TiO_2, and Pd@*g*-C_3N_4/TiO_2) are studied by SEM-EDX (Figure 5a-d) and TEM (Figure 5f-g). In SEM image of g-C_3N_4, the nanosheet structure (Figure 5b). Pure TiO_2 presents spherical-like large cauliflower-shaped particles that are non-agglomerate. Figure 5c-d shows the image of *g*-C_3N_4/TiO_2 and Pd@*g*-C_3N_4/TiO_2, respectively. Compositional analysis of prepared Pd@*g*-C_3N_4/TiO_2 catalysts was done using Energy Dispersive X-Ray Analysis (EDX). EDX results of Pd@*g*-C_3N_4/TiO_2 successfully revealed the presence of C, N, Ti, O, and Pd in the synthesized sample (Figure 5e). A transmission electron microscopy (TEM) image of the Pd@*g*-C_3N_4/TiO_2 (Figure 5f-g) nanocatalyst indicated that the presence of Pd NPs in the range of 0.04–2.5 nm with a mean diameter of 1.0 nm.

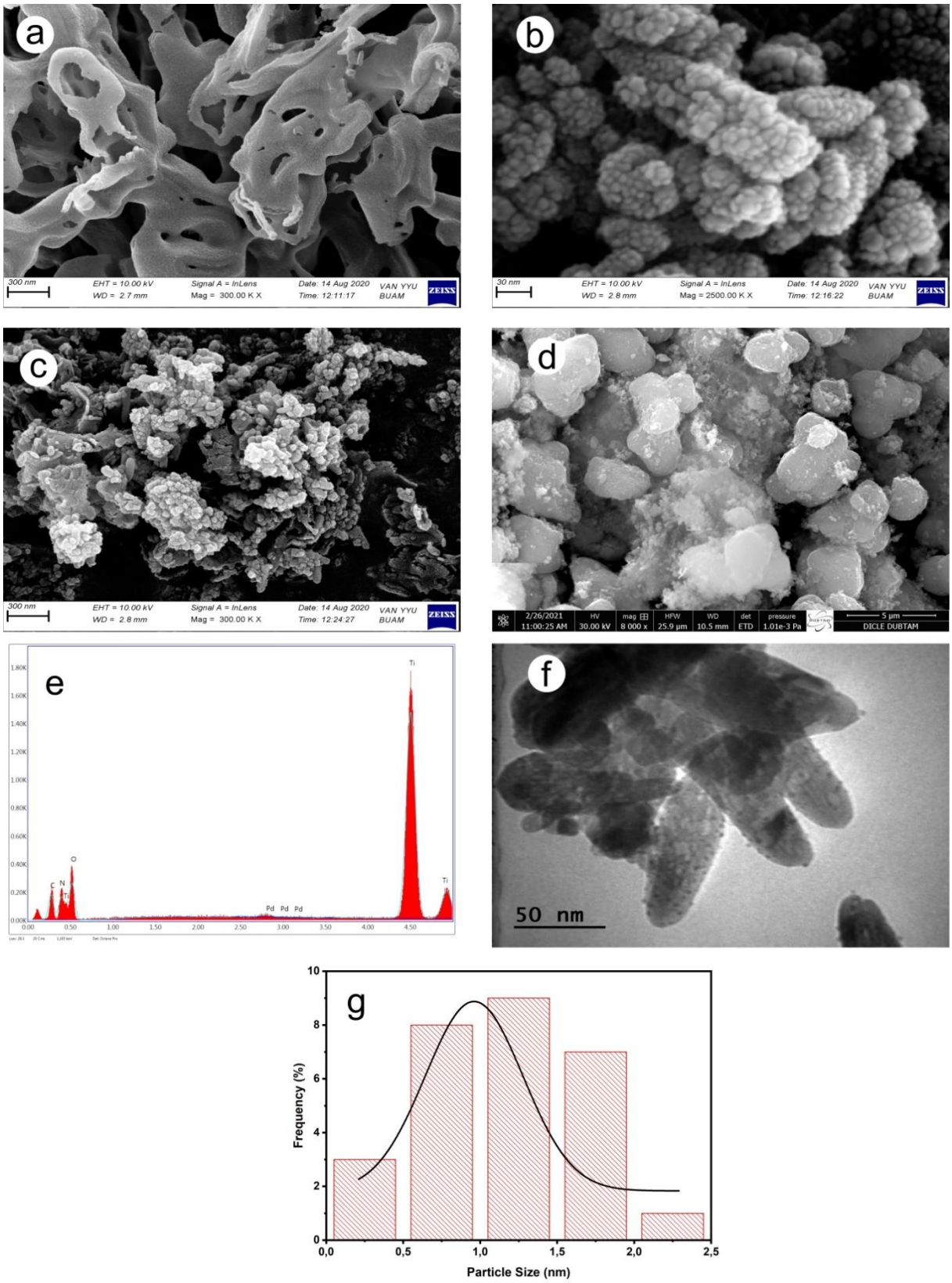

Figure 5. SEM image of a) *g*-C_3N_4 b) TiO_2 c) *g*-C_3N_4/TiO_2 and d) Pd@*g*-C_3N_4/TiO_2 e) SEM-EDX figure of Pd@*g*-C_3N_4/TiO_2 photocatalyst f) TEM image of Pd@*g*-C_3N_4/TiO_2 photocatalyst and g) size histogram of Pd NPs

3.2. Photocatalytic Activities for Methylene Blue (MB) Degradation under Visible Light Irradiation

The photocatalytic performance of Pd@*g*-C_3N_4/TiO_2 and *g*-C_3N_4/TiO_2 was assessed by determining the degradation degree of MB solution (30 mL, 7 µg/mL) under the irradiation of visible light using 0.3 %, 0.5 %, and 0.7%wt Pd (10 mg catalyst) and water as a sole solvent. As shown in Figure 6a, significant decreases in the absorption peak at 664 nm are observed in these samples, indicating that the concentration of MB in the solution is decreased. However, the Pd@g-C_3N_4/TiO_2 nanocatalyst tends to have a much faster peak descent compared to the *g*-C_3N_4/TiO_2 composite. When the *g*-C_3N_4/TiO_2 composite was used as the photocatalyst, it took 90 minutes for MB to completely degrade (Fig. 6a-b), whereas when the 0.5% wt charged Pd@*g*-C_3N_4/TiO_2 nanocatalyst was used, MB took 40 minutes to completely degrade. Also, for all these photocatalysts, the tendency of the absorption peak of MB to be blue-shifted with increasing irradiation time implies a change in the molecular structure of MB. As a result, compared with *g*-C_3N_4/TiO_2, the as-prepared Pd@*g*-C_3N_4/TiO_2 photocatalysts (0.3, 0.5, or 0.7 % wt Pd loading) showed enhanced photocatalytic performance on the degradation of MB under visible light irradiation (λ>400nm). Furthermore, to understand the reaction kinetics of the photocatalytic degradation of MB (Fig. 6b-c), the rate constant k was calculated from the equation $\ln(C_0/C_t) = kt$, and the process followed the first-order reaction. Here, C_0 and C_t are the concentrations of the MB solution at times 0 and t, respectively. The rate constant obtained from the degradation of methylene blue, as seen in Figure 6e, indicates that the reaction proceeds via pseudo-first-order kinetics. Under the irradiation of visible light, the first-order rate constants for MB degradation could be ranked as k(0.5% Pd@*g*-C_3N_4-TiO_2) >k(0.7% Pd@*g*-C_3N_4-TiO_2)> k(0.3% Pd@*g*-C_3N_4-TiO_2)> k(*g*-C_3N_4-TiO_2)(Fig. 6d). Among all catalysts, 0.5%Pd@*g*-C_3N_4-TiO_2 catalyst exhibits the highest k value. The rate constant (k) of the (0.5% Pd@*g*-C_3N_4-TiO_2) photocatalyst was approximately three times higher than that of pure *g*-C_3N_4-TiO_2. As a result, a larger k value means higher utilization efficiency of visible light, resulting in better degradation performance. In addition, the following reactions are predicted to occur during the visible light assisted photodegradation of MB dye [43].

$$\text{Catalyst} + h\nu \rightarrow h^+_{VB} + e^-_{CB} \quad (3)$$

$$h^+ + H_2O(ads) \rightarrow \bullet OH\ (ads) + H^+(ads) \quad (4)$$

$$O_2 + 2e^- \rightarrow (\bullet O^{2-})\ (ads) \quad (5)$$

$$\bullet O^{2-}\ (ads) + H^+ \leftrightarrow \bullet HO_2(ads) \quad (6)$$

$$\bullet HO_2(ads) \rightarrow H_2O_2(ads) + O_2 \quad (7)$$

$$H_2O_2(ads) \rightarrow 2\ \bullet OH\ (ads) \quad (8)$$

$$\bullet HO + MB \rightarrow CO_2 + H_2O \quad (9)$$

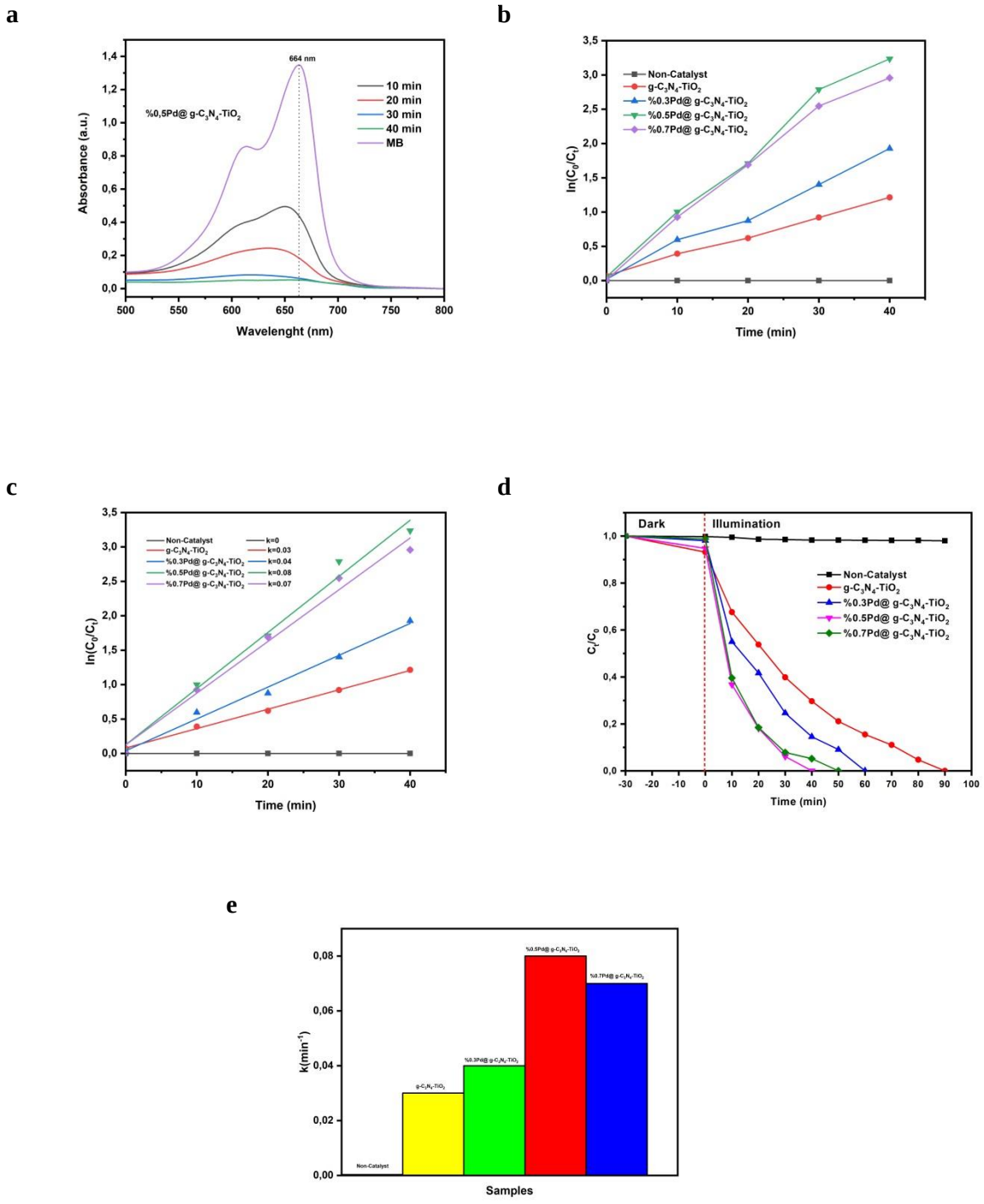

Figure 6. The degradation of MB by different photocatalysts (a) change of absorbance of MB solution (b) correlation between $\ln(C_0/C)$ with time t, (c) linear transform $\ln(C_0/C_t)$ of the kinetic curves of MB degradation d) correlation between C/C_0 with time t, e) apparent pseudo-first-order rate constant k with different catalysts.

4. Conclusions

In conclusion, we designed and successfully prepared new Pd nanoparticles, which are uniformly deposited on *g*-C_3N_4-TiO_2 through a facile method by the conventional impregnation and subsequent reduction steps. Pd@*g*-C_3N_4-TiO_2 nanocatalysts revealed a particle size of approximately 1.0 nm ±0.33 nm. We also demonstrated the characterization and use of the highly active 0.5 % wt loading Pd@*g*-C_3N_4-TiO_2 nanocatalyst for the degradation of methylene blue under visible light irradiation. The apparent rate constant for 0.5 % wt loading Pd@*g*-C_3N_4-TiO_2 is approximately three times higher than that of pure *g*-C_3N_4-TiO_2. Hence, the Pd@*g*-C_3N_4-TiO_2 as a visible light-driven photocatalyst is a promising material for the photodegradation of methylene blue in wastewater.

Acknowledgment

We would like to thank gratefully Dicle University Research Fund (*DUBAP Project No:* FEN.19.012) Diyarbakır, Turkey, for the financial support.

Ethical statement

The authors declare that this document does not require an ethics committee approval or any special permission. Our study does not cause any harm to the environment.

Declaration of Competing Interest

The authors declare no potential conflicts of interest related to the research, authorship, and publication of this article.

Authors' Contributions:

F. D: Conceptualization, Methodology, Formal analysis, Writing - Original draft preparation (50 %)

H.İ.Ö: Conceptualization, Methodology, Resources, Investigation, Writing (50 %)

All authors read and approved the final manuscript.

The compliance to Research and Publication Ethics

This work was carried out by obeying research and ethics rules.

References

[1] Akpan, U. G., Hameed, B.H., "Parameters affecting the photocatalytic degradation of dyes using TiO_2-based photocatalysts: A review", *Journal of Hazardous Materials,* 170, 520-529, 2009.

[2] Luo, X., Zhang, L., "High effective adsorption of organic dyes on magnetic cellulose beads entrapping activated carbon", *Journal of Hazardous Materials,* 171, 340-347, 2009.

[3] Zhu, M.X., Lee, L., Wang, H.H., Wang, Z., *Journal of Hazardous Materials,* 149, 735-741, 2007.

[4] Weber, E.J., Adams, R.L., *Environmental Science Technology*, 29, 1163-1170, 1995.

[5] Bruggen, B.V.D., Vandecastelee, C., Gestel T.V., Doyen W., Leysen R., *Environmental Progress,* 22, 46-56, 2003.

[6] Raghu, S., Basha, C.A., "Chemical or electrochemical techniques, followed by ion exchange, for recycle of textile dye wastewater" *Journal of Hazardous Materials,* 149, 324-330, 2007.

[7] Brillas, E., Martinez, C.A., "Decontamination of wastewaters containing synthetic organic dyes by electrochemical methods. An updated review", *Applied Catalysis B: Environmental,* 166-167, 603-643, 2015.

[8] Correira, V.M., Stephanson, T., Judd, S.J., "Characterisation of Textile Wastewaters-A Review", *Environmental Technology,* 15, 917-929, 1994.

[9] Qiu, J.H., Feng, Y., Zhang, X.F., Zhang, X.G., Jia, M.M., Yao, J.F., "Facile stir-dried preparation of g-C_3N_4/TiO_2 homogeneous composites with enhanced photocatalytic activity", *RSC Advances*, 7, 10668-10674, 2017.

[10] Wang, G.H., Xu, L., Zhang, J., Yin, T.T., Han, D., "Enhanced photocatalytic activity of powders (P25) via calcination treatment", *International Journal of Photoenergy*, 2012, 265760, 2012.

[11] Li, J.L., Jia, S.Q., Sui, G.Z., Du, L.J., Li, B.X., "Preparation of hollow Nd/TiO_2 sub-microspheres with enhanced visible-light photocatalytic activity", *RSC Advances*, 7, 34857-34865, 2017.

[12] Konstantinou, I.K., Albanis, T.A., "TiO_2-assisted photocatalytic degradation of azo dyes in aqueous solution: kinetic and mechanistic investigations: A review", *Applied Catalysis B: Environmental*, 49, 1-14, 2004.

[13] Teh, C.Y., Wu, T.Y., Juan, J.C., "An application of ultrasound technology in synthesis of titania-based photocatalyst for degrading pollutant", *Chemical Engineering Journal*, 317, 586-612, 2017.

[14] Teh, C.Y., Wu, T.Y., Juan, J.C., "Facile sonochemical synthesis of N,Cl-codoped TiO2: Synthesis effects, mechanism and photocatalytic performance", *Catalysis Today*, 256, 365-374, 2015.

[15] Ullah, R., Dutta, J.,"Photocatalytic degradation of organic dyes with manganese-doped ZnO nanoparticles", *Journal of Hazardous Materials*, 156,194-200, 2008.

[16] Zhang, G., Gao, Y., Zhang, Y., Guo, Y., "Fe_2O_3-Pillared Rectorite as an Efficient and Stable Fenton-Like Heterogeneous Catalyst for Photodegradation of Organic Contaminants", *Environmental Science Technology*, 44, 6384-6389, 2010.

[17] Li, X., Zhu, J., Li, H., "Comparative study on the mechanism in photocatalytic degradation of different-type organic dyes on SnS_2 and CdS", *Applied Catalysis B: Environmental*, B 123, 174-181, 2012.

[18] Gong, D.G., Highfield, J.G., Ng, S.Z.E., Tang, Y.X., Ho, W.C.J., Tay, Q.L., Chen, Z., "Poly Tristriazines as visible light sensitizers in Titania-based composite photocatalysts: Promotion of Melon development from urea over acid Titanates", *ACS Sustainable Chemistry & Engineering*, 2, 149–157, 2014.

[19] Wang, X., Maeda, K., Thomas, A., Takanabe, K., Xin, G., Carlsson, J.M., Domen, K., Antonietti, M., "A metal-free polymeric photocatalyst for hydrogen production from water under visible light", *Nature Materials.* 8, 76–80, 2009.

[20] Li, Y.N., Wang, M.Q., Bao, S.J., Lu, S.Y., Xu, M.W., Long, D.B., Pu, S.H.. "Tuning and thermal exfoliation graphene-like carbon nitride nanosheets for superior photocatalytic activity", *Ceramics International*, 42, 18521-18528, 2016.

[21] Chen, Y., Wang, X.C., "Template-free synthesis of hollow g-C_3N_4 polymer with vesicle structure for enhanced photocatalytic water splitting", *The Journal of Physical Chemistry C*, 122, 3786-3793, 2018.

[22] Li, J.L., Liu, T., Sui, G.Z., Zhen, D.S., "Photocatalytic performance of a Nd-SiO_2-TiO_2 nanocomposite for degradation of Rhodamine B dye wastewater", *Journal Nanoscience And Nanotechnology*, 15, 1408-1415, 2015.

[23] Wang, J., Wang, G.H., Wei, X.H., Liu, G., Li, J., "ZnO nanoparticles implanted in TiO_2 macrochannels as an effective direct Z-scheme heterojunction photocatalyst for degradation of RhB", *Applied Surface Science*, 456, 666-675, 2018.

[24] Zhou, W., Li, W., Wang, J.Q., Qu, Y., Yang, Y., Xie, Y., Zhang, K.F., Wang, L., Fu, H.G., Zhao, D.Y., "Ordered mesoporous black TiO_2 as highly efficient hydrogen evolution photocatalyst", *Journal of the American Chemical Society*, 136, 9280-9283, 2014.

[25] Thompson, T.L., Yates, J.T., "Surface science studies of the photoactivation of TiO_2-New photochemical processes", *Chemical Reviews*., 38, 4428-4453, 2006.

[26] Tong, Z.W., Yang, D., Xiao, T.X., Tian, Y., Jiang, Z.Y., "Biomimetic fabrication of g-C_3N_4/TiO_2 nanosheets with enhanced photocatalytic activity toward organic pollutant degradation", *Chemical Engineering. Journal*, 260, 117-125, 2015.

[27] Lu, N., Wang, C.Y., Sun, B., Gao, Z.M., Su, Y., "Fabrication of TiO_2-doped single layer graphitic-C_3N_4 and its visible-light photocatalytic activity", *Separation And Purification Technology*., 286, 226-232, 2017.

[28] Tan, Y.G., Shu, Z., Zhou, J., Li, T.T., Wang, W.B., Zhao, Z.L., "One-step synthesis of nanostructured g-C_3N_4/TiO_2 composite for highly enhanced visible-light photocatalytic H_2 evolution", *Application Catalyst B-environmental*., 230, 260–268, 2018.

[29] Li, J.L., Du, L.J., Jia, S.Q., Sui, G.Z., Zhang, Y. L., Zhuang, Y., Li, B.X., Xing, Z.Y.. "Synthesis and photocatalytic properties of visible light-responsive, three-dimensional, flower-like La–TiO_2/g-C_3N_4 heterojunction composites", *RSC Advances*, 8, 29645-29653, 2018.

[30] Das, T. K., Banerjee, S., Vishwanadh, B., Joshi, R., Sudarsan, V., "On the nature of interaction between Pd nanoparticles and C_3N_4 support", *Solid State Sciences*, 83, 70–75, 2018.

[31] Ming Lei, Zhiying Wang, Lihua Zhu, Wenshan Nie, Heqing Tang, "Complete debromination of 2,2′,4,4′-tetrabromodiphenyl ether by visible-light photocatalysis on g-C_3N_4 supported Pd", *Applied Catalysis B: Environmental*, 261, 118-236, 2020.

[32] Hosseini S. M., Ghiaci M., Farrokhpour H., "The adsorption of small size Pd clusters on a g-C_3N_4 quantum dot: DFT and TD-DFT study", *Materials Research Express*, 6(10), 105079, 2019.

[33] Guo Y., Xiao L., Zhang M., Li Q., Yang J., "An oxygen-vacancy-rich Z-scheme g-C_3N_4/Pd/TiO_2 heterostructure for enhanced visible light photocatalytic performance, *Applied Surface Science*, 440, 432–439, 2018.

[34] R.A. Senthil, J. Theerthagiri, A. Selvi, J. Madhavan, "Synthesis and characterization of low-cost g-C_3N_4/TiO_2 composite with enhanced photocatalytic performance under visible-light irradiation", *Optical Materials*, 64, 533-539, 2017.

[35] R.A. Senthil, J. Theerthagiri, A. Selvi, J. Madhavan, "Synthesis and characterization of low-cost g-C_3N_4/TiO_2 composite with enhanced photocatalytic performance under visible-light irradiation", *Optical Materials*, 64, 533-539, 2017.

[36] Çelebi, M., Yurderi, M., Bulut A., Kaya, M., Zahmakıran, M., "Palladium nanoparticles supported on amine-functionalized SiO_2 for the catalytic hexavalent chromium reduction" *Applied Catalysis B: Environmental*, 180, 53-64, 2016.

[37] Yan, H., Yan, H., "TiO_2–g-C_3N_4 composite materials for photocatalytic H_2 evolution under visible light irradiation", *Journal of Alloys and Compounds*, 509, 26- 29, 2011.

[38] Sabri, N.A., Nawi, M.A., Nawawi, W.I., "Porous immobilized C coated N doped TiO_2 containing in-situ generated polyenes for enhanced visible-light photocatalytic activity", *Optical Materials*, 48, 258-266, 2015.

[39] Zhang, Q., Meng, G., Wu, J., Li, D., Liu, Z., "Study on enhanced photocatalytic activity of magnetically recoverable Fe_3O_4@C@TiO_2 nanocomposites with core-shell nanostructure", *Optical Materials*, 46, 52-58, 2015.

[40] R.A. Senthil, J. Theerthagiri, A. Selvi, J. Madhavan, "Synthesis and characterization of low-cost g-C_3N_4/TiO_2 composite with enhanced photocatalytic performance under visible-light irradiation", *Optical Materials*, 64, 533-539, 2017.

[41] Yu Y., Zhao Y., Huang T., Liu H., "Shape-controlled synthesis of palladium nanocrystals by microwave irradiation", *Pure Applied Chemistry*, 81, 2377-2385, 2009.

[42] Ghorbani S., Parnian R., Soleimani E. "Pd nanoparticles supported on pyrazolone-functionalized hollow mesoporous silica as an excellent heterogeneous nanocatalyst for the selective oxidation of benzyl alcohol", *Journal of Organometallic Chemistry*, 952, 122025, 2021.

[43] Rauf, M. A., & Ashraf, S. S., "Fundamental principles and application of heterogeneous photocatalytic degradation of dyes in solution", *Chemical engineering journal*, 151 (1-3), 10-18, 2009.